Controlled Particle Growth of Silver Sols through the Use of Hydroquinone as a Selective Reducing Agent

Stuart T. Gentry,*[,†] Stephen J. Fredericks,[†] and Robert Krchnavek[‡]

Department of Chemistry and Biochemistry, La Salle University, 1900 West Olney Avenue, Philadelphia, Pennsylvania 19141, and College of Engineering, Rowan University, 201 Mullica Hill Road, Glassboro, New Jersey 08028

Received July 29, 2008

Hydroquinone (HQ) was used as the principal chemical reducing agent to prepare aqueous silver nanocolloids from silver nitrate. The data demonstrate that HQ is unable to initiate the particle growth process on its own, but is able to sustain particle growth in the presence of pre-existing metallic clusters. This unique selectivity is similar to that seen in photographic systems. Data are presented on two different approaches to initiating the HQ growth process. Very low levels of sodium borohydride can be used to form seed particles. Alternatively, the data show that controlled growth can be initiated by exposing the samples to UV radiation, relying on the photoreactivity of hydroquinone to start the process. These results were used to explore the dynamics of very dilute $NaBH_4$ seed particles. They also were used to create nonspherical disk and triangular-plate morphologies directly from solution, without the need for subsequent reformation or template processing.

Introduction

Interest in sub 100 nm systems is not a recent phenomenon. More than a century before "nanotechnology" entered the public lexicon, Michael Faraday published work on the unique optical properties seen with gold nanosols.[1] It was almost 100 years later that published work began to appear to explain the synthesis of these colloids, and in particular to explain their remarkable uniform particle size distributions.[2−4] Today there are a wide variety of catalytic, biologic, and optical applications that make use of the unique properties seen with nanocolloids.[5−8]

Despite the extensive work done on these systems, there remains a great deal of interest in the preparation and dynamics of particle growth. The growth model originally proposed by LaMer[3] described early reduction of isolated atoms, followed by burst nucleation of a supersaturated solution into particle seeds. He then described continued diffusion-controlled atom addition onto those primary particles as the principle mode of particle growth. He argued that particle−particle coalescence would not yield the narrow particle size distributions seen in many nanocolloids. The more common approach in recent years is to consider surface addition to be in kinetic and thermodynamic competition with particle−particle aggregation.[9−11] Given the wide variety of modern experimental systems, it should be no surprise that there is a wide variability in how well the current data fit the early LaMer model.

In this paper we intend to help shed additional light on the dynamics of particle growth. One of the perennial problems is separating particle growth from continued particle nucleation. We will discuss a synthetic process that cleanly separates the two. The system exploits the chemistry of photographic developers—making use of the known phenomenon where hydroquinone (HQ) is unable to reduce isolated silver ions in a photographic film, but is able to reduce silver in those same films when in the presence of previously photogenerated metallic clusters. We will show that hydroquinone is an effective reducing agent for growing out silver particles, but only if seed particles are already present. These seed particles can be created by adding a small amount of strong chemical reducing agent such as sodium borohydride (at levels as low as 0.0002 mole fraction relative to the silver concentration). Alternatively, particle growth can be initiated by utilizing the photoactivity of hydroquinone that is known from biological systems.

Irrespective of whether one uses photoinitiation or chemical-seed formation to start the process, once the seed is formed hydroquinone can be used on its own to add additional silver atoms directly to the growing seeds. Hydroquinone, however, is unable to start new particles even though it continues to grow out existing particles. It is this forced selectivity which makes the HQ system different from other published seeded processes.[12−14]

Surface Plasmon Theory. The explanation for the unique optical properties demonstrated by gold and silver nanocolloids is now well understood. In 1908, Mie proposed a general solution to the problem of spherical particles interacting with an external electromagnetic field.[15] His equations in combination with the Drude free-electron model can be used to show that small particles develop a surface polarization charge due to an applied optical EM field.[16] A key simplification for Mie theory is the case where the particles are much smaller than the wavelength of light. This "dipole approximation" allows one to assume that the optical electric field is constant across the full width of the particle. The

† La Salle University.
‡ Rowan University.

(1) Faraday, M. *Philos. Trans. R. Soc. London* **1857**, *147*, 145.
(2) Turkevich, J.; Stevenson, J.; Hillier, P. C. *J. Discuss. Faraday Soc.* **1951**, *11*, 55.
(3) LaMer, V. K.; Dinegar, R. H. *J. Am. Chem. Soc.* **1950**, *72*, 4847.
(4) Reiss, H. *J. Chem. Phys.* **1951**, *19*, 482.
(5) Yguerabide, J.; Yguerabide, E. E. *Anal. Biochem.* **1998**, *262*, 137–157.
(6) Edwards, P. P.; Thomas, J. M. *Angew. Chem., Int. Ed.* **2007**, *46*, 2.
(7) R.F. Aroca, R. F.; Alvarez-Puebla, R. A.; Pieczonka, N.; Sanchez-Cortez, S.; Garcia-Ramos, J. V. *Adv. Colloid Interface Sci.* **2005**, *116*, 45.
(8) Kerker, M. *J. Colloid Interface Sci.* **1985**, *105*, 297.
(9) Watzky, M. A.; Finke, R. G. *J. Am. Chem. Soc.* **1997**, *119*, 10382.
(10) Park, J.; Privman, V.; Matijevič, E. *J. Phys. Chem. B* **2001**, *103*, 11630.
(11) Van Hyning, D. L.; Kemperer, W. G.; Zukoski, C. F. *Langmuir* **2001**, *17*, 3128.
(12) Cao, L.; Zhu, T.; Liu, Z. *J. Colloid Interface Sci.* **2006**, *293*, 69.
(13) (a) Jana, N. R.; Gearheart, L.; Murphy, C. J. *Adv. Mater.* **2001**, *13*, 1389. (b) Jana, N. R.; Gearheart, L.; Murphy, C. J. *J. Phys. Chem. B* **2001**, *105*, 4065.
(14) Yu, H.; Gibbons, P. C.; Kelton, K. F.; Buhro, W. E. *J. Am. Chem. Soc.* **2001**, *123*, 9198.
(15) Mie, G. *Ann. Phys.* **1908**, *25*, 377.
(16) Link, S.; El-Sayed, M. A. *J. Phys. Chem. B* **1999**, *103*, 8410.

10.1021/la803680h CCC: $40.75
Published on Web 02/09/2009

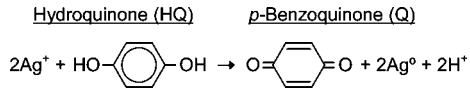

Figure 1. Simplified hydroquinone oxidation scheme.

small size also allows one to assume that free electrons are more likely to be scattered by the surface of the particle than by bulk effects such as lattice defects or phonon scattering. The result of applying these approximations is that the composite free-electron cloud in small particles can be thought of as oscillating back and forth with the applied electric field. This creates a temporary excess of surface charge on one side of the particle and a reversal of charge on the opposite side. The optical energy absorbed by this oscillation reaches a maximum at a characteristic resonant plasmon wavelength. The practical result of Mie theory is that, for silver particles smaller than about 40 nm in diameter, an optical experiment will show a strong, sharp extinction peak that is located at 380−420 nm depending on the surface chemistry and surrounding medium. This peak is the result of a combination of both absorption and scattering due to light interactions with the plasmon field.

Reduction of Silver Ions to Silver Metal. A number of schemes have been used to generate gold and silver sols. Common to all of the systems is that (A) the noble metal must be reduced to its metallic form and (B) these aggregated metallic atoms must be able to form a stable sol. This latter criterion usually requires that a stabilizing agent be present to inhibit the irreversible coagulation of particles with one another.

Faraday originally used phosphorus to reduce gold ions to gold metal.[1] Since then, the most common reducing agents used for sol formation have been sodium citrate[17] and sodium borohydride.[18,19] Other chemical reducing agents that have been used with silver include amines,[20] alcohols,[21] phosphines,[22] and even geranium plant extract.[23]

The current work uses HQ as the reducing agent (Figure 1). It was chosen because of its unique selectivity. It is able to reduce silver onto metallic particles that are already present but is unable to reduce silver when the ions are isolated in solution. It also has the practical advantage of having manageable kinetics; i.e., it can be formulated to reduce $AgNO_3$ in anywhere from 5 to 15 min at room temperature depending on the formulation conditions. HQ generates a low level of steric stabilization for the colloids, but is nevertheless a poor surface stabilizer due to the weak binding of hydroquinone and quinone to silver sols. This can be used to separate the reducing agent from stabilization effects when one is interested in exploring the efficiency of different surfactants and stabilizers.

Experimental Section

Sample Preparation. All chemicals were reagent grade and used as received from the supplier without additional purification. Water was deionized and passed through a 0.22 μm filter. Glassware was soaked in concentrated HNO_3 and rinsed multiple times in water. Unless otherwise stated, a standard formulation was a 15 mL solution of 0.2 mM silver nitrate (Aldrich, prepared as a 1.0×10^{-3} M stock solution), 0.2 mM hydroquinone (Aldrich, prepared fresh each day as a 5.0×10^{-2} M solution), and 0.2 mM sodium citrate as a colloidal stabilizer (prepared as a 1.0×10^{-3} M stock solution), with dilution to full volume with water. The samples were buffered using a 0.6 mM 1:1 (mol/mol) mixture of potassium phosphate, monobasic (JT Baker), and sodium phosphate, dibasic (Mallinckrodt). The poly(vinylpyrrolidone) (MP Biomedicals) used in this work had a molecular weight of 40 000. The order of addition was such that the water and buffer were combined first followed by addition of the $AgNO_3$ and citrate. The HQ was added last, and timing was started on the addition of the reducing agent. For those samples that were prepared by the $NaBH_4$-seeded process, we used a 4.0×10^{-4} M borohydride solution prepared fresh each day and kept chilled in ice−water. The $NaBH_4$ was added after the buffer, $AgNO_3$, and sodium citrate were mixed. The borohydride was usually allowed to react and sit for 2−3 min prior to addition of the HQ. However, adding the HQ prior to the $NaBH_4$ addition did not appear to significantly influence the results. All reported mole fraction concentrations are relative to the starting concentration of $AgNO_3$.

Instruments. The majority of the plasmon extinction spectra (particularly those showing the time development for particle growth) were recorded using an Ocean Optics, Inc. USB4000 CCD linear-array spectrometer system. The light source was an Ocean Optics ISS-UV/vis, which utilizes a 3.8 W deuterium bulb and 1.2 W tungsten bulb. A Unicam UV4 UV/vis spectrometer was used to obtain high-definition extinction spectra. These instruments were run in absorption mode, but they were actually extinction measurements since particle plasmons simultaneously absorb and scatter incident light. Excitation spectra were obtained using a Hitachi F-4500 fluorescence spectrometer. This instrument uses a 150 W xenon lamp as its excitation source. Samples exposed to broad-band UV excitation used an Ultraviolet Products Inc. Mineralight UVS-54 hand-held UV lamp (6 W), with the sample introduced into a quartz cuvette and then set 4 in. from the lamp.

Particle size data were collected using a Brookhaven 90Plus dynamic light scattering instrument provided by Rowan University. This device uses time-correlated light scattering to extract diffusion coefficients and then calculates concomitant particle sizes. It was run using 658 nm incident radiation. Size distributions were calculated using a non-negative constrained least-squares (NNLS) routine. Reported diameters are volume-weighted averages. Scanning electron micrographs were collected using Rowan University's Leo 1530VP scanning electron microscope. Colloidal samples were allowed to evaporate on a conductive silicon wafer and were typically viewed using a 2−4 kV beam.

Bright-field transmission electron micrographs were recorded using a Phillips CM12 scanning/transmission electron microscope at the USDA's Eastern Regional Research Center. Samples were evaporated on carbonized copper grids, and the microscope was operated at 80 kV. Particle sizes were determined by analyzing the micrographs using ImageJ, a Java program developed at the National Institute of Mental Health (rsb.info.nih.gov/ij).

Results

Dékány and co-workers previously presented work that used HQ to form silver nanocolloids.[24] The focus of their work was on kinetics rather than their choice of HQ. The written text of their work implies a simple reaction between silver and reducing agent. They make no mention of the critical need to initiate the process with UV exposure or a preseeded colloid. It is possible that their success at making colloids was the result of the fortuitous particularities of their equipment. Their system was exposed to continuous UV radiation by leaving their samples in a broad-band UV/vis spectrometer beam while collecting extinction data as a function of time. It should be noted that this lack of discussion of the underlying electrochemistry does not detract from their specific results. The electrochemistry does impact, however, the

(17) Lee, P. C.; Meisel, D. J. *J. Phys. Chem.* **1982**, *86*, 3391.
(18) Creighton, J. A.; Blatchford, C. G.; Albrecht, M. G. *J. Chem. Soc., Faraday Trans. 2* **1979**, *75*, 790.
(19) Van Hyning, D. L.; Zukoski, C. F. *Langmuir* **1998**, *14*, 7034.
(20) Brown, K. R.; Natan, J. J. *Langmuir* **1998**, *14*, 726.
(21) Silvert, P. Y.; Herrera-Urbina, R.; Tekaia-Elhsissen, K. *J. Mater. Chem.* **1997**, *7*, 293.
(22) Chen, Z.; Gao, L. *Mater. Res. Bull.* **2007**, *42*, 1657.
(23) Richardson, A.; Janiec, A.; Chan, B. C.; Crouch, R. D. *Chem. Educ.* **2006**, *11*, 331.
(24) (a) Patakfalvi, R.; Dékány, I. *J. Therm. Anal. Calorim.* **2005**, *79*, 587. (b) Patakfalvi, R.; Virányi, Z.; Dékány, I. *Colloid Polym. Sci.* **2004**, *283*, 299. (c) Patakfalvi, R.; Papp, S.; Dékány, I. *J. Nanopart. Res.* **2007**, *9*, 353.

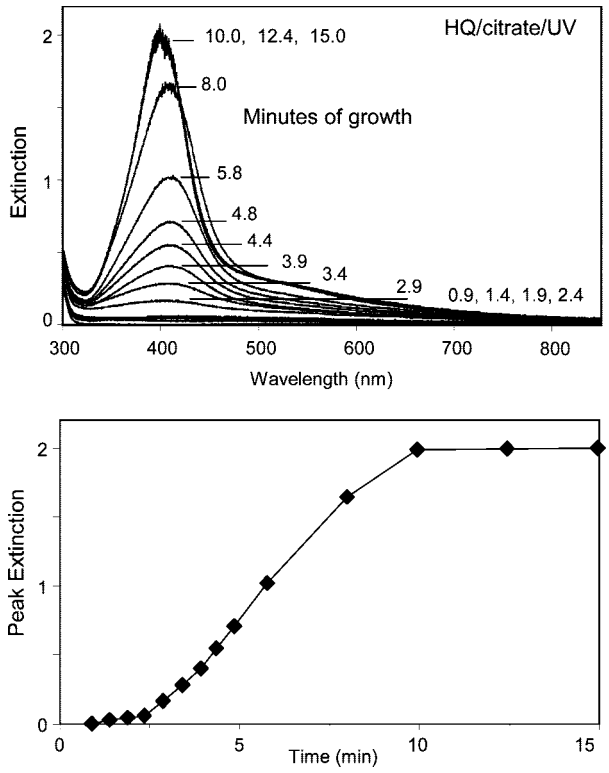

Figure 2. Extinction spectra of a sample containing 0.2 mM $AgNO_3$, 0.2 mM sodium citrate, and 0.2 mM HQ. The sample was exposed to UV light for the duration of the experiment.

extension of their experimental procedure to other systems as well as the elucidation of the various chemical mechanisms at play in their system.

Using the HQ/citrate system along with photoinitiation by UV light, it is possible to generate silver nanosols. Figure 2 shows a typical plasmon spectrum during the growth process. It also quantifies the growth by plotting the peak extinction as a function of time. An induction period is seen at early times (<2 min), followed by rapid growth at later times. (The specifics of this system and the resulting particle size distributions will be discussed later in this paper.)

HQ Selectivity. HQ is a unique reducing agent for silver as witnessed by its long use as a photographic developer. It is well accepted in the photographic industry that HQ is successful as a developer because it is selective in reducing silver ions. It is unable to reduce *isolated* silver ions in photographic film but is able to reduce silver ions when they are in the presence of pre-existing *metallic clusters*. These clusters must be at least four atoms in size.[25,26] In the photographic process, exposure of the AgBr film to light creates small metallic clusters, but the clusters are too small to be visible to the naked eye in a photographic negative. The subsequent HQ developer step is a dark process that amplifies (grows) the metallic clusters by adding additional Ag atoms to the nascent clusters to make them more visible while selectively leaving the unexposed film unchanged (unreacted).

The reason for this selectivity is that the redox potential for reducing isolated silver ions is markedly different than when adding to metallic clusters (Table 1). The redox potential for hydroquinone ($E° = -0.7$ V) is unable to overcome the highly negative redox potential of isolated silver (−1.8 V), but is sufficient to reduce silver onto stable clusters or onto solid Ag electrodes (+0.8 V).

Table 1. Redox Potential as a Function of the Silver Cluster Size[27−29]

$Ag^+ + 1e^- \rightarrow Ag°$	$E° = -1.8$ V vs NHE
$Ag^+ + Ag°_3 + 1e^- \rightarrow Ag°_4$	$E° = -0.9$ V
$Ag^+ + Ag°_4 + 1e^- \rightarrow Ag°_5$	$E° = -0.4$ V
$Ag^+ + Ag°_\infty + 1e^- \rightarrow Ag°_\infty$	$E° = +0.799$ V
$Q + 2H^+ + 2e^- \rightarrow HQ$	$E° = -0.699$ V
	$E = -0.3$ V at pH 7[a]
general range for photographic developers[28]	$E = -0.2$ to -0.5 V

[a] The redox potential for Q → HQ is pH dependent due to the presence of H^+ on the quinone side of the equation. The Nernst equation can be used to adjust the potential for this pH effect.[30]

This same photographic electrochemistry controls the system when the use of HQ is extended to the formation of nanocolloids. The specific redox potentials shift when switching from photographic AgBr films to aqueous $AgNO_3$ solutions. Nevertheless, the HQ reducing agent is still selective to reducing Ag^+ in the presence of nucleated $Ag°_n$ seeds while being unreactive to isolated ions.

Seeded Process Using $NaBH_4$

Given that HQ needs pre-existing Ag clusters to reduce Ag^+ ions, there are several possible strategies for initiating those clusters. One is to use a very small amount of strong reducing agent such as $NaBH_4$ to seed the process and then use HQ to finish the growth. Figure 3 compares the extinction spectrum of $AgNO_3$/HQ/sodium citrate solutions that were prepared with and without the preaddition of $NaBH_4$ as a preliminary reducing agent. Figure 4 is a transmission electron micrograph of a resultant seeded sample similar to that in Figure 3b.

The unseeded colloid in Figure 3a demonstrates that if HQ is the *sole reducing agent*, it is unable to react with Ag^+ on its own; there is no visible plasmon peak at 400 nm even if it is allowed to sit overnight in the dark at room temperature. However, if a small amount of $NaBH_4$ is first put into the $AgNO_3$ solution as in Figure 3b, then HQ is able to reduce all the remaining Ag^+.

The borohydride in Figure 3b quickly reacted with aqueous silver ions, but there was only enough BH_4^- present to react with a small fraction of the Ag^+ ions in solution. The resultant borohydride-created particles were stable and did not grow further once the BH_4^- in solution was exhausted and the system reached equilibrium. The redox reaction only resumed once additional reducing agent in the form of HQ was added. Since clusters of metallic silver were now present, any HQ added at this point was able to react with the large amount of remaining ionic silver and finish off the reaction. The presence of the seed clusters shifted the redox potential of the silver to a point that was sufficient to allow HQ to participate. In other words, HQ served as an effective reducing agent once $NaBH_4$ had been used to start the process, but HQ was unable to form initial $Ag°_n$ seeds on its own. We anticipate that this same process should hold true with other strong chemical reducing agents beyond $NaBH_4$.

(25) Fayet, P.; Granzer, F.; Hegenbart, G.; Moisar, E.; Pischel, B.; Wöste, L. *Phys. Rev. Lett.* **1985**, *55*, 3002.
(26) Leisner, T.; Rosche, Ch.; Wolf, S.; Granzer, F.; Wöste, L. *Surf. Rev. Lett.* **1996**, *3*, 1105.
(27) Linnert, T.; Mulvaney, P.; Henglein, A.; Weller, H. *J. Am. Chem. Soc.* **1990**, *112*, 4657.
(28) Mostafavi, M.; Marignier, J. L.; Amblard, J.; Belloni, J. *Radiat. Phys. Chem.* **1989**, *34*, 605.
(29) Henglein, A. *Top. Curr. Chem.* **1988**, *143*, 113.
(30) Ives, D. J. G.; Jan, G. J. In *Reference Electrodes: Theory and Practice*; Ives, D. G., Janz, G. J., Eds.; Academic Press: New York, 1961; Chapter 6.

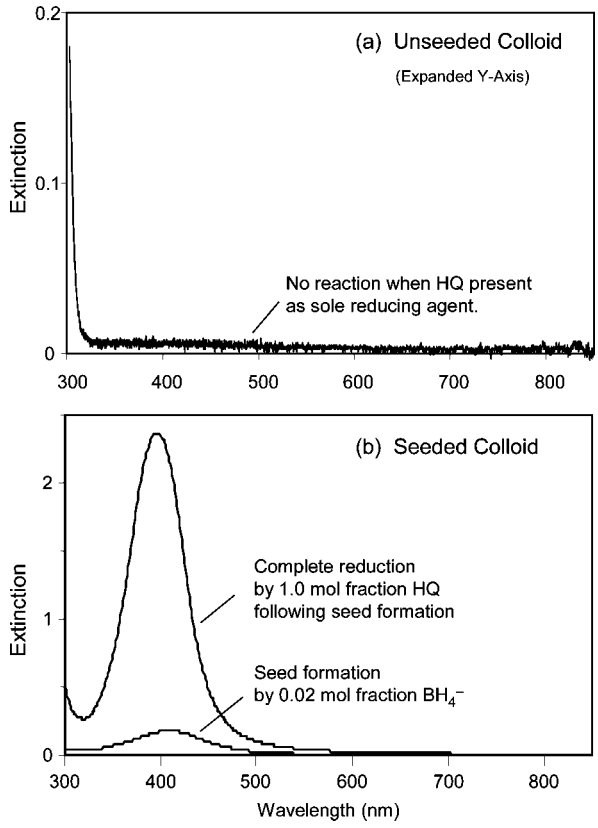

Figure 3. Extinction spectra on unseeded and seeded samples. The unseeded colloid contained 1.0 mole fraction HQ relative to the number of moles of $AgNO_3$, but no $NaBH_4$. The seeded colloid was initially charged with 0.02 mole fraction $NaBH_4$. HQ (1.0 mole fraction) was added to the seeded sample after 3 min. All samples contained 0.2 mM $AgNO_3$ and 0.2 mM sodium citrate. (No external ultraviolet light was used.)

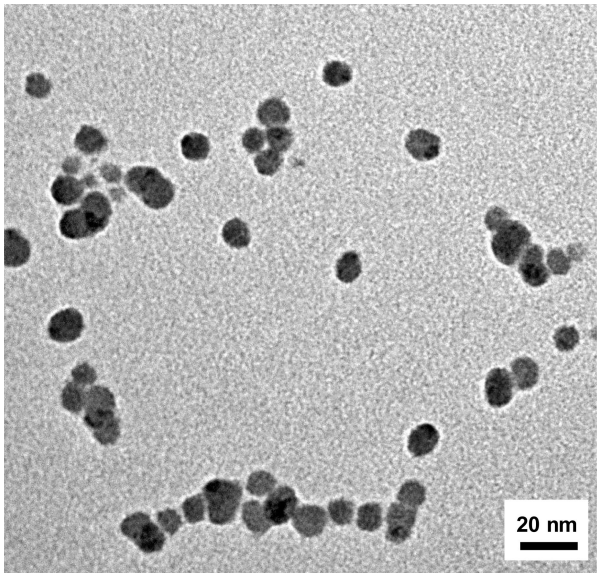

Figure 4. TEM image of the sample prepared using the seeded process—0.2 mM $AgNO_3$, 0.2 mM sodium citrate, and 0.020 mole fraction $NaBH_4$, followed by a 2 min hold and then a second stage of 0.2 mM HQ.

Further Comments on $NaBH_4$ for the Seeded Process. Each molecule of sodium borohydride has the potential to provide up to 8 electrons for redox reactions. There are a number of possible oxidative pathways for BH_4^-, but a typical end product in a neutral vs alkaline aqueous environment is boric acid or borohydroxide:[31,32]

$$BH_4^-(aq) \rightarrow H_3BO_3(aq) \rightarrow B(OH)_4^-(aq) \qquad (1)$$

In practice, it has been reported by Shirtcliffe et al.[33] and verified in this laboratory that BH_4^- is more likely to offer a maximum of between 5 and 7 electrons per $NaBH_4$ in a pH-neutral colloid rather than the theoretically possible 8 electrons. Figure 5 shows that, at low levels of $NaBH_4$, all of the available reducing agent is consumed by excess $AgNO_3$. If the BH_4^- level is increased at dilute concentrations, then the peak extinction steadily increases as more of the silver is able to be reduced. However, if the level of $NaBH_4$ continues to be increased beyond its stoichiometric limit, then $NaBH_4$ switches from being the limiting reagent to being the excess reagent and the peak extinction reaches a plateau based on the $AgNO_3$ concentration. This switch in limiting reagents extrapolates to a $NaBH_4$ mole fraction of ca. 0.23—or 7.0 electrons out of the maximum 8 electrons available per $NaBH_4$.

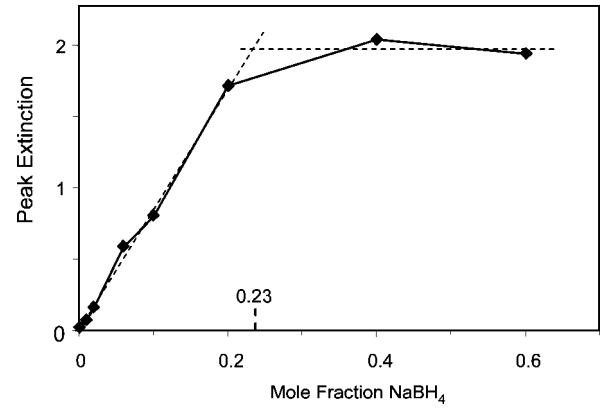

Figure 5. Peak extinction as a function of the $NaBH_4$ mole fraction (relative to $AgNO_3$). The samples also contained 1.0 mole fraction sodium citrate but no HQ.

The 0.02 mole fraction $NaBH_4$ used in the seeding experiment in Figure 3 was well below the limiting amount of 0.23 mole fraction seen in Figure 5. This verifies that the borohydride used in Figure 3 was only able to react with a small fraction of the available Ag^+ present, leaving the remaining silver ions available to react later with the HQ. This was also seen visually in that the sample in Figure 3 remained just slightly colored after the seed formation and only demonstrated the typical intense yellow plasmon color after HQ was added to grow out the particles.

Figure 3 used a relatively high nucleating concentration of 0.02 mole fraction $NaBH_4$ for illustration purposes. However, even $NaBH_4$ levels 100 times lower (0.0002 mole fraction) were able to initiate the HQ reduction reaction and allow HQ to overcome the redox potential barrier seen with isolated Ag^+ ions.

In summary, even though very low levels of $NaBH_4$ are only able to reduce a small fraction of the available Ag^+ ions, those reactions are critical for allowing HQ to reduce the rest of the silver ions. With even a small amount of $NaBH_4$ present, HQ is able to create a large plasmon signal by reducing the remaining silver ions present in solution, but if no BH_4^- is present, then no sol is formed.

(31) Herne, T. M.; Garrell, R. L. *Anal. Chem.* **1991**, *63*, 2290.

(32) Davis, R. E.; Bromes, E.; Kirby, C. L. *J. Am. Chem. Soc.* **1962**, *84*, 885.

(33) Shirtcliffe, N.; Nickel, U.; Schneider, S. *J. Colloid Interface Sci.* **1999**, *211*, 122.

Table 2. Particle Size as a Function of $NaBH_4$ Preaddition (As Measured Using an Optical Particle Size Analyzer)

BH_4^- preadded concn[a] (mole fraction)	HQ postadded concn[a] (mole fraction)	av particle diam (nm)	calcd seed diam (nm)
0.002	1.0	26	6
0.005	1.0	25	8
0.01	1.0	18	8
0.02	1.0	13	7
0.05	1.0	10	7
0.1	1.0	1	1
0.005	1.0, HQ	25	8
0.005	0.2, $NaBH_4$	7	NA

[a] Concentrations relative to the number of moles of $AgNO_3$ present. HQ has a theoretical maximum of 2 equiv/mol. BH_4^- has a theoretical maximum of 8 equiv/mol.

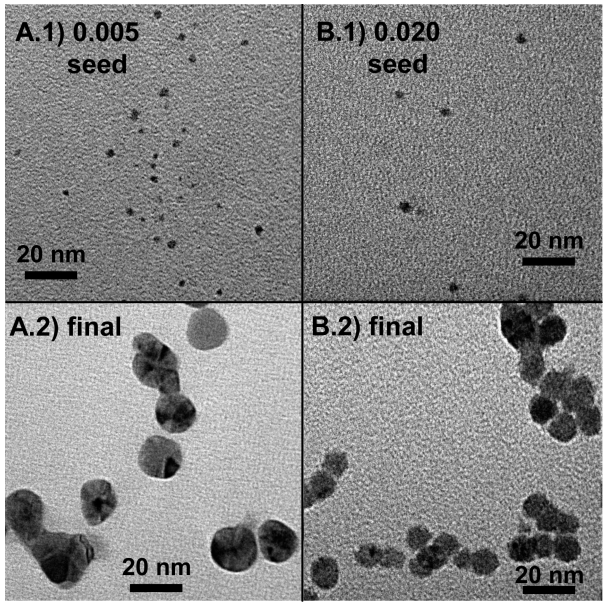

Figure 6. TEM images taken of seeded samples before and after the second stage of HQ was added. Sample A used a 0.005 mole fraction BH_4^- seed, with A.1 and A.2 taken before and after the HQ. Sample B used a 0.020 mole fraction BH_4^- seed, with B.1 and B.2 taken before and after the HQ. All samples were prepared with 0.2 mM $AgNO_3$, 0.2 mM sodium citrate, and 0.6 mM phosphate buffer. Average particle sizes as determined by optical imaging software on multiple micrographs were (sample A.1) 3.3 nm, (sample A.2) 14.1 nm, (sample B.1) 3.3 nm, and (sample B.2) 10.2 nm.

Application of HQ to Particle-Growth Studies of the Seeded Process

Previously in this paper we asserted that the unique electrochemical selectivity of HQ could be used to explore particle-growth dynamics. An example of this utility can be seen when the final particle size as a function of the $NaBH_4$ seed concentration is studied. Table 2 presents particle diameter data as the seed concentration of $NaBH_4$ was varied across a range of values. These experiments were conducted by mixing $AgNO_3$, sodium citrate (as a stabilizer), phosphate buffer (pH 7), and a specified low level of $NaBH_4$ as a first stage. The system was then held for 2 min to allow for complete reaction and equilibration of the borohydride. (There was no change in result when using longer hold times.) After the hold period, hydroquinone was added in an excess amount to allow for complete reduction of the remaining $AgNO_3$. The system was then allowed to sit for 15 min to allow for full particle growth. A separate set of samples were also run using a second addition of $NaBH_4$ following initial seed formation rather than using HQ for the second stage. Figure 6 shows representative micrographs for similar samples.

Table 2 lists the average particle diameter as determined by the particle size analyzer. (The weighted averages were determined from the distributions calculated by the NNLS software. See the Supporting Information for full distributions.) The table also includes calculated diameters for the initial *seed* particles based on the final diameters and the mole fraction of BH_4^- present relative to $AgNO_3$. These calculations assume (1) HQ only adds silver atoms to existing particles, with no nucleation of additional particles, (2) the volume change from seed to final particle is therefore due to the ratio of the number of initial Ag atoms reduced by BH_4^- compared to the remaining Ag atoms that were later reduced by HQ, and (3) a borohydride efficiency of 7:1 for the number of Ag atoms reduced by each formula unit of BH_4^- (as determined earlier in this paper).

All of the calculated seed diameters (with one exception) fall in the range of 6−8 nm irrespective of a 25-fold difference in the dilute amounts of $NaBH_4$ present. Furthermore, using 0.2 mole fraction $NaBH_4$ in the second stage to finish off the grow-out rather than using HQ in the second stage gave the same 7−8 nm diameter as the initial seeds. The one exception to these results was the 0.10 mole fraction BH_4^-/1.0 mole fraction HQ data point. It is assumed that this was an instrumental artifact, but we do not have the data at this time to declare this with certainty.

The constancy of the seed particle size is worth noting. This particle size was independent of concentration, suggesting thermodynamic equilibrium rather than a kinetic effect. Furthermore, this stable seed state was reached even in the case of 0.002 mole fraction $NaBH_4$ relative to $AgNO_3$. Given the highly reactive nature of $NaBH_4$ as a reducing agent, it can be reasonably assumed that all of the initial charge of BH_4^- was immediately consumed by the dilute system. This means that no excess BH_4^- was present to help facilitate resolubilization and subsequent redeposition of silver to reach the preferred size. The same particle size was also achieved when using two separate additions of $NaBH_4$ rather than forming the colloid from a single solution. This implies the second $NaBH_4$ addition caused additional nucleation and reformation. All of these observations are quite different from the historical LaMer model that used initial saturation limits and competing kinetics to explain the tight size control seen in silver sols.[3] Among other things, the LaMer model predicts that, once particles begin to form, even BH_4^- systems will only add preferentially to growing particles and should not start additional clusters. This is clearly not the case in our work where the only way that the second sequential addition of BH_4^- could give the same final particle size of 7 nm as the original seed is if the second addition created its own set of new particles. This suggests that the resultant size is the result of thermodynamic equilibrium that depends in part on the other chemical species present in the system.

The particle size analyzer data in Table 2 can be compared to the micrographs in Figure 6 (additional micrographs with larger coverage are included in the Supporting Information). The exact numeric results do not match, but the qualitative trends hold. Both techniques showed that the diameter of the seed particles was independent of the level of BH_4^- used to form the seed. The micrographs gave average diameters for the seed particles of 3 nm for both the 0.005 and 0.020 mole fraction BH_4^-samples (as compared to particle size analyzer diameters of 8 and 7 nm, respectively). Both techniques also showed that the samples with the lower levels of BH_4^- ultimately grew out to larger sizes than the samples with more concentrated BH_4^-

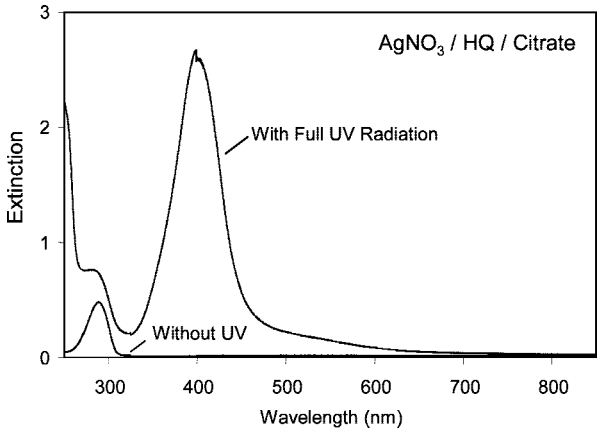

Figure 7. HQ reaction with and without UV radiation. The sample contained 0.2 mM $AgNO_3$, 0.2 mM sodium citrate, and 0.2 mM HQ. The sample was exposed to UV radiation for 15 min.

seeds. The micrograph diameters for the fully grown samples were 10 and 14 nm for the 0.005 and 0.020 mole fraction BH_4^- samples (as compared to 10 and 25 nm for the light-scattering data). There are a number of reasons for the differences in numeric values between the two techniques including the assumptions that go into extracting particle sizes from optical light-scattering equipment, TEM issues with calibration and focus when the available equipment is pushed to its resolution limit, and samples prepared at different times and with different lots of raw materials. In spite of these issues, what is seen with both techniques is that the particle sizes of the seeds are constant irrespective of the amount of $NaBH_4$ used to generate the seeds. The two techniques also show that, once the BH_4^- seeds are generated, those systems with less BH_4^- (and therefore a lower number of seed particles) grow into larger particles than those systems grown out with seeds made from higher BH_4^-concentrations.

These comments on particle grow-out have focused on the interaction of $AgNO_3$ with $NaBH_4$. The observations, however, were made possible by relying on the unique characteristics of HQ as a selective reducing agent. The concentrations of seed particles generated by the dilute $NaBH_4$ samples were so low as to make the initial colloids appear colorless to the eye and below the sensitivity of our optical equipment. The value of the HQ selectivity was in the ability to take these very dilute samples and then grow them to more observable sizes in a controlled and predictable manner without initiating any new particles.

Photoinitiated Reaction Process

In the preceding section we demonstrated that a chemical reducing agent such as $NaBH_4$ can be used to nucleate a metallic seed and enable subsequent HQ reaction. There are other possible routes for initiating the HQ reaction. Ultraviolet radiation can be used to convert HQ to an excited electronic state where it is then sufficiently energetic to drive the reduction of isolated $Ag^+ \rightarrow Ag°$.

Figure 7 shows a representative UV-initiated plasmon spectrum for a $AgNO_3$/HQ/citrate sample. The system did not contain any $NaBH_4$ but instead was exposed to UV light to initiate the process. The system produced a strong surface plasmon peak at 400 nm. This same system did not demonstrate any particle growth when it was left in the dark or only exposed to ambient room light. This was true even when the sample was allowed to sit for 2 days in the dark following mixing.

Figure 8 is a TEM image taken of a sample made under the same full-UV conditions as in Figure 7. As can be seen in the

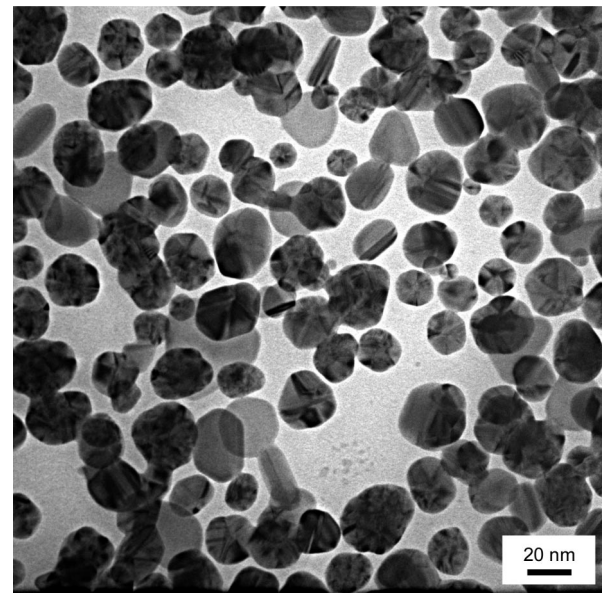

Figure 8. TEM image of the sample prepared using the UV-assisted process—0.2 mM $AgNO_3$, 0.2 mM sodium citrate, and 0.2 mM HQ, exposed to a broad-band UV source.

micrograph, the UV-initiated process does suffer from poorer particle size control than the BH_4^--seeded process. (See the Supporting Information for particle size distributions of seeded vs UV-initiated samples.) However, most of the particles from the UV process are still less than 40 nm in diameter, which is the upper limit needed for the silver plasmon resonance to remain at a wavelength of 400 nm. Thus, the spectrum in Figure 7 is nicely peaked at 400 nm but has a long tail at red-shifted wavelengths due to the subset of particles larger than 40 nm.

This photoinitiated reaction does not require a large optical power density to drive the nucleation process. In fact, even the small amount of radiation resulting from leaving a sample in a low-power continuous-exposure photodiode-array spectrometer is sufficient to start the reaction. (It was this type of exposure that was fortuitously present in the previously mentioned Dékány work.[24]) In practice, however, our more general procedure was to use a small portable UV lamp to provide uniform exposure to the entire cuvette, removing the sample from the lamp only long enough to insert and capture data in the linear-array spectrometer before returning the sample to the lamp. Alternatively, a fluorescence spectrometer was used in its excitation mode to measure particle growth as a function of the specific excitation wavelength.

Wavelength Dependence of Photoinitiation. The wavelength of the excitation radiation is a critical parameter for the photoinitiated process. Early experiments with glass cutoff filters demonstrated that the radiation must be UV rather than visible light. We then undertook a more careful examination of the photoinitiation wavelength. Rather than using a broad-band UV source, we used the excitation wavelength selectivity of a fluorescence spectrometer to select a narrow bandwidth of optical radiation. Figure 9 shows the peak values for the plasmon extinction (at 400−425 nm depending on the sample) as a function of the excitation wavelength (210−310 nm) and for different exposure times. The figure demonstrates that particle growth and plasmon generation reach maximum rates at excitation wavelengths of ca. 230 and 290 nm. These peaks coincide with

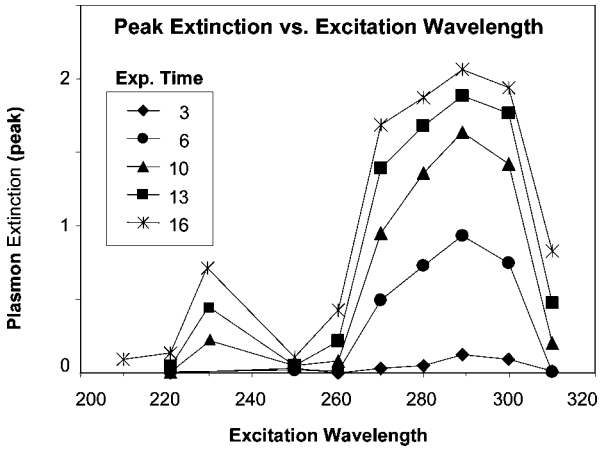

Figure 9. Peak plasmon extinction as a function of the excitation wavelength. The samples all contain 0.2 mM $AgNO_3$, 0.2 mM HQ, and 0.2 mM sodium citrate. The extinction was also monitored as function of the exposure time.

the 290 and 221 nm absorption peaks reported in the literature and seen in our laboratory for aqueous HQ.[34]

There is a wealth of information available on the photoreactivity of quinoid compounds,[35] albeit with much of the focus being on starting reactants of *p*-benzoquinone and naphthoquinone due to their importance in biological systems. Studies have shown that photo-oxidation of hydroquinone typically proceeds through a pathway of optical excitation of the first singlet transition ($\pi-\pi^*$), followed by intersystem crossing and relaxation to a longer lived triplet state ($\tau = 0.9\ \mu s$), and then diffusion-controlled redox reactions involving semiquinone intermediates.[36] This is consistent with our data in Figure 9.

It should be noted that this UV initiation is quite different from the optical plasmon-excitation growth reported by other research groups.[37−39] Researchers have used existing seed particles and then applied direct excitation to the surface plasmons at wavelengths of 400 nm or longer to induce further growth on the particles. Their data are reported to be due in part to coupling of the plasmon electric field with the growth process. In our case, we are irradiating samples at much shorter wavelengths than normal plasmonic transitions and in systems that do not start with any particles present and hence do not initially have any plasmonic fields to couple with the radiation.

Plasmon Development as a Function of the UV Exposure Time. As with the $NaBH_4$-seeded process, UV exposure can be used to initiate the process and then turned off so that the remaining HQ reaction can proceed on its own. All that is required is that a minimum level of particle nucleation must have occurred before removal of the UV source.

Figure 10 shows plasmon spectra for samples receiving a variety of durations of UV exposure, ranging from 15 s to full exposure for 15 min. In all cases the samples were allowed to continue to grow in the dark after being removed from the UV source. All of the samples show full development of the plasmon signal,

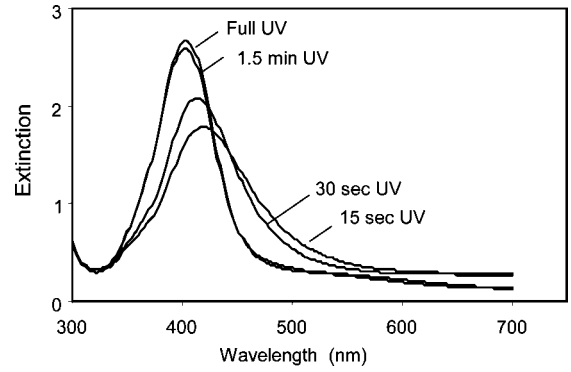

Figure 10. Extinction spectra for the $AgNO_3$/HQ/citrate sample immediately after 1.5 min of broad-band UV exposure as well as after 15 min of additional aging without UV exposure.

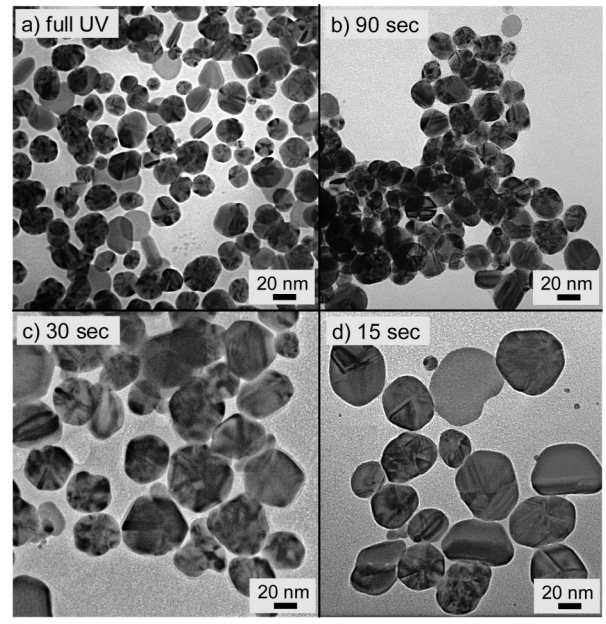

Figure 11. TEM images for samples exposed to (a) full UV exposure or (b) 90 s, (c) 30 s, or (d) 15 s of UV exposure followed by 15 min of grow-out time in the dark.

although the bandwidth begins to degrade with shorter exposure times. Figure 11 provides TEM micrographs for the samples in Figure 10, and Figure 12 shows the time development of peak extinction for various exposure times.

The data show that if a sample is exposed to UV radiation for at least 1.5 min, then one can obtain well-defined plasmon peaks even if the remainder of the particle grow-out occurs in the dark. Shortening the exposure to less than 1 min still gives fully developed particles, but the plasmon peaks are broader in width and less intense. The micrographs in Figure 11 demonstrate that all of the samples give a range of particle sizes. In the case of the longer exposure times, however, those ranges in particle diameters are still primarily less than the 40 nm upper limit necessary to hold the peak resonance at 400 nm wavelength. As the exposure time is decreased, the average size gets larger, leading to an increasing number of particles having diameters in excess of 40 nm.

These observations are qualitatively consistent with what was seen with the much more controlled BH_4^--seeded process. The UV exposure creates initial seeds that HQ can then add to through its selective reduction capabilities. The fact that the longer UV exposure times give smaller final particles indicates that the UV

(34) Kurien, K. C.; Robins, P. A. *J. Chem. Soc. B* **1970**, 855.
(35) Itoh, T. *Chem. Rev.* **1995**, *95*, 2351.
(36) (a) Linschitz, H.; Rennert, J.; Korn, T. M. *J. Am. Chem. Soc.* **1954**, *76*, 5839. (b) Feitelson, J.; Shaklay, N. *J. Phys. Chem.* **1967**, *71*, 2582. (c) Bridge, N. K.; Porter, G. *Proc. R. Soc. London, A* **1958**, *244*, 259. (d) Pan, Y.; Fu, Y.; Yu, H.; Gao, Y.; Guo, Q.; Yu, S. *J. Phys. Chem. A* **2006**, *110*, 7316. (e) Boule, P.; Rossi, A.; Pilichowski, J. F. *New J. Chem.* **1992**, *16*, 1053.
(37) Jin, R. C.; Cao, Y. W.; Mirkin, C. A.; Kelly, K. L.; Schatz, G. C.; Zheng, J. G. *Science* **2001**, *294*, 1901.
(38) Zheng, Z.; Xu, W.; Corredor, C.; Xu, S.; An, J.; Zhao, B.; Lombardi, J. R. *J. Phys. Chem. C* **2007**, *111*, 14962.
(39) Maillard, M.; Huang, P.; Brus, L. *Nano Lett.* **2003**, *3*, 1611.

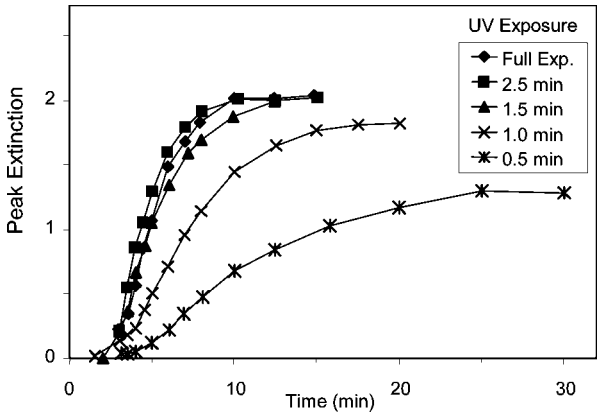

Figure 12. Peak extinction as a function of the development time for $AgNO_3$/HQ/citrate samples after varying amounts of UV exposure. The data include a 30 s delay between mixing and starting the exposure. Peak widths at 15 min were 75, 75, 78, 87, and 153 nm for the full, 2.5 min, 1.5 min, 1.0 min, and 0.5 min UV exposure times, respectively.

radiation continues to initiate new particle growth for the entire time that the sample is exposed to the UV radiation. An increased number of seed particles means that any one of the growing particles receives less of the remaining unreacted silver and hence remains smaller in size. It can also be noted that unlike the BH_4^-system, there does not appear to be significant thermodynamic redistribution of silver to form uniform particle sizes. This is concluded from the large span of sizes present in the final colloids.

Application of HQ To Control Particle Morphology

The unique properties of hydroquinone as a selective reducing agent can also be utilized to prepare nonspherical particle morphologies. Researchers have reported a variety of colloidal silver morphologies including rods, oblate spheroids, and triangular plates.[37,39−42] The procedures for making these shapes often requires a long (multihour or several days) reformation cycle where the system forms initial particles and then with continued processing relies on Ostwald ripening to redistribute and reshape the atoms found in the original particles. Another approach is to use micellar templates to guide particle formation.[13] As will be shown, the selective nature of the HQ electrochemistry allows for nonspherical particles to be grown directly from the initial process in a matter of minutes without any additional reformation or templates required.

We used the $NaBH_4$/HQ two-stage seeded process, with the only differences from previously cited samples being the choice of stabilizer, when that stabilizer is added, the concentration of the seed, and the pH of the system. Figure 13 shows representative scanning electron micrographs for samples made under varying conditions, and Figure 14 shows the corresponding optical extinction data. The figures show the morphology can be manipulated by changing the stabilizer system, with resultant morphologies ranging from spherical particles to a mixture of spheres and disks and last to triangular plates. These morphological changes in turn lead to changes in plasmon extinction spectra as the anisotropic shapes give rise to bimodal transverse and red-shifted longitudinal scattering peaks.[43]

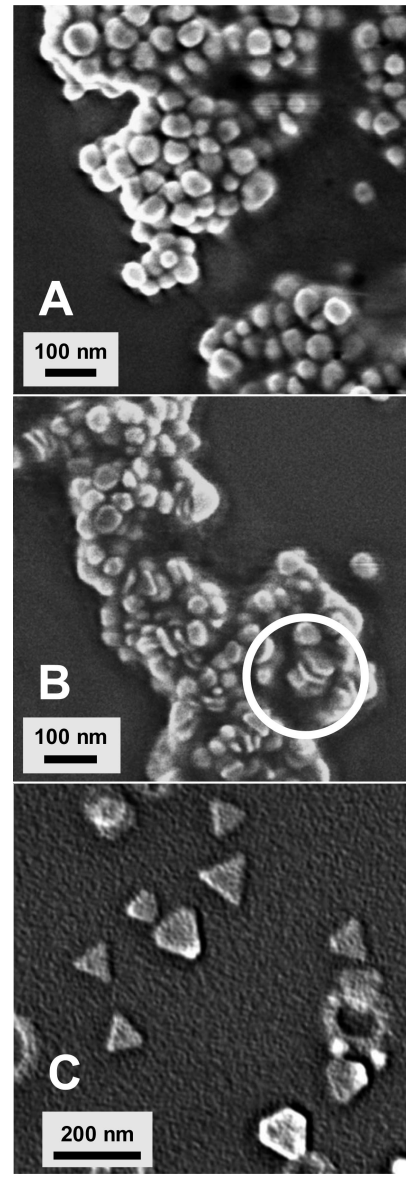

Figure 13. Scanning electron micrographs of colloids made from 0.002 mole fraction $NaBH_4$ followed by second-stage addition of 1.0 mole fraction HQ. Samples differ in the stabilizer added to the first stage: (A) no additional stabilizer; (B) 1.0 mole fraction sodium citrate; (C) 0.20 wt % poly(vinylpyrrolidone).

Evidence for the direct formation of nonspherical morphologies is seen in Figure 15, which looks at a buffered poly(vinylpyrrolidone) (PVP) sample as a function of time. The figure clearly shows early development of a bimodal extinction spectrum that is characteristic of nonspherical particles. The increasing red shift with time in the downfield peak is due to the expansion of the longitudinal dimensions as more and more of the silver ions are reduced onto the edges of the growing plates. This is in contrast to previously reported methods of synthesizing nonspherical particles that typically involve an initial step of forming normal, spherical particles followed by additional processing to allow those particles to reform into other thermodynamic shapes.

In a subsequent paper we will provide a more detailed study of this morphological control. What is important for this current paper is the general conclusion that the forced single-atom growth onto existing particles with the selective HQ reducing agent provides a level of particle-growth control not typically achievable with other systems. This can be manipulated to control the

(40) Sosa, I. O.; Noguez, C.; Barrera, R. G. *J. Phys. Chem. B* **2003**, *107*, 6269.
(41) Zhao, L. L.; Kelly, K. L.; Schatz, G. C. *J. Phys. Chem. B* **2003**, *107*, 7343.
(42) Jing, A.; Tang, B.; Ning, X.; Zhou, J.; Xu, S.; Zhao, B.; Weiqing, X.; Corredor, C.; Lombardi, J. R. *J. Phys. Chem. C* **2007**, *111*, 18055.
(43) Kelly, K. L.; Coronado, E.; Zhao, L. L.; Schatz, G. C. *J. Phys. Chem. B* **2003**, *107*, 668.

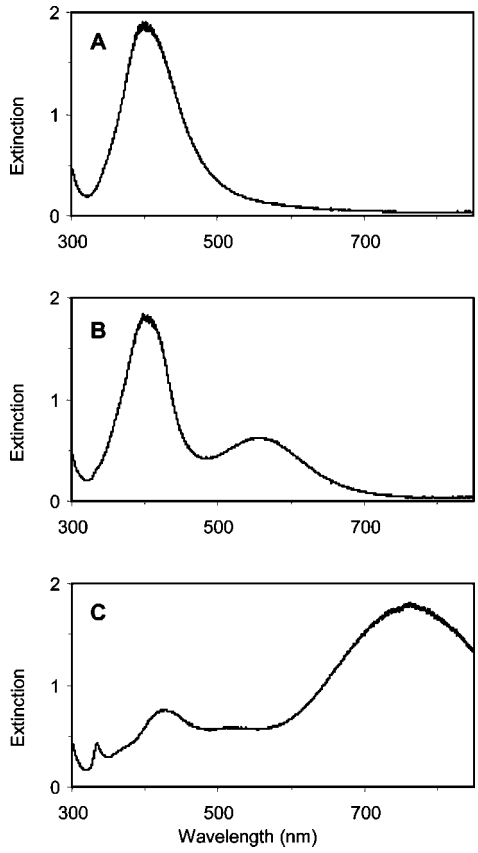

Figure 14. Extinction spectra for the colloids shown in Figure 13. Samples differ in the stabilizer added to the first stage: (A) no additional stabilizer; (B) 1.0 mole fraction sodium citrate; (C) 0.20 wt % poly(vinylpyrrolidone).

morphology through thermodynamic rather than kinetically controlled growth.

Conclusions

The experiments incorporated in this study demonstrate some of the unique properties that can be attributed to using HQ as a reducing agent when preparing silver nanocolloids. The experimental system demonstrates selectivity to silver that is similar to that present in photographic developer systems; HQ is unable to reduce isolated silver ions but is able to reduce those same ions when added onto pre-existing silver metallic clusters. This phenomenon can be used to explore differences in nucleation versus growth mechanisms. It can also be used to control particle morphologies.

In this study we demonstrate different ways that particle nucleation can be initiated prior to HQ growth. $NaBH_4$ can be used as a complementary reducing agent. If the borohydride is added at very low levels (as low as 0.0002 mole fraction relative to the $AgNO_3$ concentration), then BH_4^- is quickly consumed,

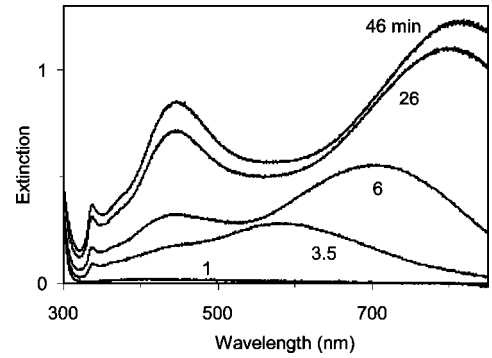

Figure 15. Extinction spectra for the system containing 0.002 mole fraction $NaBH_4$, 0.2 wt % poly(vinylpyrrolidone), 1.0 mole fraction HQ, buffer, and 0.2 mM $AgNO_3$. $AgNO_3$, the buffer, and $NaBH_4$ were combined, PVP was then added and the resulting solution allowed to sit for 7 min, and then finally HQ was added. Times in the figure are relative to HQ addition.

generating small seed particles but leaving the large majority of the silver as unreacted ions. Once seed particles are present, HQ can be used to reduce the remaining silver and grow the particles to their full size. It was found that changing the starting $NaBH_4$ concentration changed the number of seed particles present, but not the size of the seed particles. This change in the number of particles controlled the final size of the fully developed colloids.

In this study we also show that UV light can be used to initiate the HQ growth process. This photoinitiation is optimized when using 289 nm light to excite the first singlet transition in HQ, which ultimately leads to triplet oxidation. Like with the BH_4^--seeded process, the UV radiation can be used to start the process by creating nascent particles, and then the radiation can be removed to allow HQ to finish the particle growth on its own in the dark. Shortening the exposure time gives larger final particles, which is consistent with there being less photogenerated seed particles. This implies that new particles continue to be generated for the full duration of UV exposure. A consequence of this ongoing nucleation, however, is that the photogenerated particles lack the tight size uniformity seen with the BH_4^--seeded process.

Acknowledgment. We acknowledge the help and access to instrumentation offered by Rowan University. We also are appreciative of the use of the transmission electron microscope and guidance by Dr. Peter Cooke at the USDA Eastern Regional Research Laboratory. Last, we acknowledge the many helpful discussions with Dr. Michael Prushan of La Salle University.

Supporting Information Available: Additional experimental data for the particle size distribution for samples prepared via the seeded process and via the UV-initiated process. This material is available free of charge via the Internet at http://pubs.acs.org.

LA803680H